Low recycling and high power density handling physics in the Current Drive Experiment-Upgrade with lithium plasma-facing components[a)]

R. Kaita,[b)] R. Majeski, T. Gray, H. Kugel, D. Mansfield, J. Spaleta,
J. Timberlake, and L. Zakharov
Princeton Plasma Physics Laboratory, Princeton, New Jersey 08543

R. Doerner and T. Lynch
University of California at San Diego, La Jolla, California 92093

R. Maingi
Oak Ridge National Laboratory, Oak Ridge, Tennessee 37831

V. Soukhanovskii
Lawrence Livermore National Laboratory, Livermore, California 94550

The Current Drive Experiment-Upgrade [T. Munsat, P. C. Efthimion, B. Jones, R. Kaita, R. Majeski, D. Stutman, and G. Taylor, Phys. Plasmas **9**, 480 (2002)] spherical tokamak research program has focused on lithium as a large area plasma-facing component (PFC). The energy confinement times showed a sixfold or more improvement over discharges without lithium PFCs. This was an increase of up to a factor of 3 over ITER98P(y,1) scaling [ITER Physics Basis Editors, Nucl. Fusion **39**, 2137 (1999)], and reflects the largest enhancement in confinement ever seen in Ohmic plasmas. Recycling coefficients of 0.3 or below were achieved, and they are the lowest to date in magnetically confined plasmas. The effectiveness of liquid lithium in redistributing heat loads at extremely high power densities was demonstrated with an electron beam, which was used to generate lithium coatings. When directed to a lithium reservoir, evaporation occurred only after the entire volume of lithium was raised to the evaporation temperature. The ability to dissipate a beam power density of about 60 MW/m^2 could have significant consequences for PFCs in burning plasma devices. © 2007 American Institute of Physics. [DOI: 10.1063/1.2718509]

I. INTRODUCTION

For fusion to be a practical energy source, among the outstanding issues that need to be addressed is the nature of the "first wall" that will face thermonuclear plasmas. The high power densities and large neutron fluxes that plasma-facing components (PFCs) must handle for long periods of time pose a difficult challenge for conventional solid materials. For this reason, liquid metals have been suggested as an alternative approach to fusion reactor PFCs.[1] Radiation damage will not be an issue for liquid metal PFCs, and since they can flow, they are able to dissipate high heat loads. Furthermore, material eroded as a consequence of either normal operation or disruptions will be replaced by new material.

Experience with significant quantities of circulating alkali metals in nuclear power applications dates at least as far back as the French SuperPhenix reactor about 20 years ago.[2] Before they could be considered for a large magnetic confinement fusion (MCF) device, it was realized that experiments were needed on a modest scale to address safe handling issues, and the liquid metal magnetohydrodynamic (MHD) effects arising from the complex, time-varying magnetic fields found in the MCF environment. These studies, together with the investigation of the interaction of magnetically confined plasmas with liquid metal PFCs, became the primary research focus of the Current Drive Experiment-Upgrade (CDX-U) spherical tokamak.

The liquid metal chosen for CDX-U was lithium. In addition to its consideration as a candidate material for a breeding blanket in a fusion reactor, it has the attractive feature of being the least reactive of the alkali metals. At the same time, the ability of lithium to bind hydrogen chemically means that it can be a low recycling PFC.[3] The effect of such a PFC on improving plasma performance was demonstrated on the Tokamak Fusion Test Reactor (TFTR), in which lithium was deposited on limiter surfaces by a variety of means.[4] Furthermore, theoretical studies have predicted that with low recycling, flat temperature profiles can be achieved. The stable confinement regimes that result could lead to substantial improvements in ITER-scale plasmas.[5]

The CDX-U experiments have demonstrated the benefits of lithium as a PFC. Section II of this article describes the device, including its various capabilities for lithium PFC experiments. Section III discusses the ability of liquid lithium to dissipate heat in the presence of high power densities.[6] New calculations are presented that show how this could be explained by convective flows established in the lithium in CDX-U. Section IV focuses on the effects of lithium PFCs on plasma fueling that, to the authors' knowledge, have not been reported previously. This includes a discussion of the density evolution after the termination of plasma fueling, and its relation to different recycling conditions. The achieve-

---
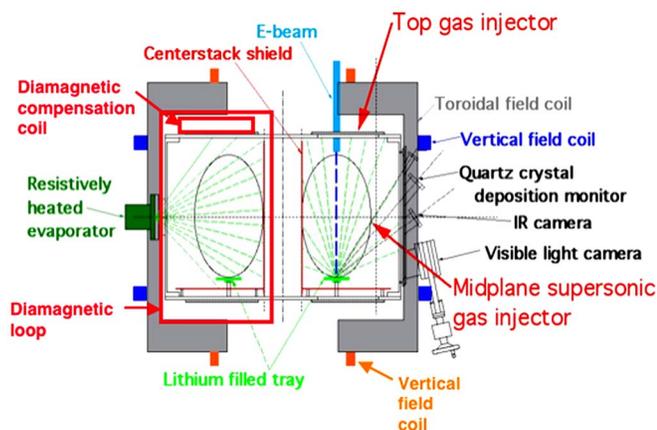
FIG. 1. (Color online) Cross section of CDX-U with components related to plasma fueling, diagnostics, and lithium PFCs.
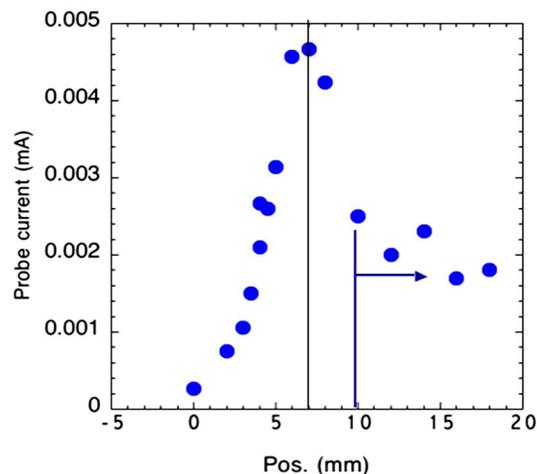

FIG. 2. (Color online) Electron beam profile determined from current probe measurements. Note that the distortion of the profile beyond 10 mm is due to beam deflection from charge accumulation on the probe insulator.

ment of high energy confinement times in plasmas with lithium PFCs are also summarized in this section.[7] Section V describes the suppression of MHD instabilities in CDX-U liquid lithium limiter plasmas. Their absence is one of the most conspicuous features of these discharges, and this result has not been published until now. The paper concludes, in Sec. VI, with a summary and comments on future liquid lithium PFC research on a successor to CDX-U, the Lithium Tokamak Experiment (LTX).

II. DESCRIPTION OF CDX-U

An elevation of CDX-U is shown in Fig. 1, with the plasma indicated schematically inside the vacuum vessel. Discharges typically had a major radius of 34 cm and a minor radius of 22 cm, resulting in a low aspect ratio of about 1.5. For the experiments described in this paper, the maximum plasma current was about 80 kA. Central electron temperatures were in the 100 eV range, and the line-averaged densities were between 0.5×10^{19} and 1×10^{19} cm^{-3}. Figure 1 also depicts the outer "legs" of the toroidal field coils, which were designed to be detachable from the center stack. The toroidal field on axis was kept at 2.1 kG during the final CDX-U run period.

The lithium PFC experiments on CDX-U were performed with a combination of a fully toroidal liquid lithium limiter and wall coatings from lithium evaporators. To form the limiter, liquid lithium was contained in a stainless steel tray mounted near the bottom of the vacuum vessel (Fig. 1).[8] The tray was centered at the plasma major radius of 34 cm, and it had two toroidal electrical breaks. A channel 10 cm wide and 0.64 cm deep was used to contain the lithium, and it was kept in liquid form with resistive heaters mounted beneath the tray.

Two techniques were used to evaporate lithium onto the CDX-U vacuum vessel walls for the experiments described here. They involved a resistively heated "oven" containing lithium, and an electron beam (e-beam) that evaporated lithium in the limiter tray. The "line-of-sight" trajectories from the two lithium sources are shown in Fig. 1. They were able to produce lithium coatings up to 10 and 100 nm thick,

respectively, as measured with a quartz crystal deposition monitor (QDM) in a 1-min interval preceding the discharge (Fig. 1). The QDM was physically located behind a gate valve on the nipple shown in Fig. 1. The axis of the nipple was normal to the face of the QDM crystal.

III. POWER HANDLING CAPABILITIES OF LIQUID LITHIUM

The e-beam evaporator approach also demonstrated the effectiveness of liquid lithium in dissipating extremely high heat loads. Between plasma shots, the set of vertical field coils nearest to the CDX-U midplane in Fig. 1, along with the toroidal field coils, were used to guide the e-beam to the lithium in the limiter tray. The e-beam width was obtained from the current drawn by a probe that was scanned across the beam (Fig. 2). The charge that built up on the probe insulator disturbed the e-beam and distorted the data at the end of the scan. It was still possible to determine, however, a profile width of approximately 3 mm. This meant that when the e-beam was operated at high power, there was a very localized deposition of about 1.5 kW, or 60 MW/m^2, on the lithium in the limiter tray. Significant lithium evaporation occurs between 400 °C and 500 °C, and if conduction was the only means of dissipating the e-beam power, this temperature range should have been reached within tens of milliseconds.

In the e-beam evaporation experiment, only part of the tray was filled. This is depicted in the upper part of Fig. 3, along with the spot where the e-beam was directed. The location of several thermocouples are also shown. The sensors labeled 1 and 3 are the two nearest to the beam spot, and are most sensitive to the bulk lithium temperature. However, they are still about 30° toroidally, or 18 cm in arc length away. Note that the abscissa for the plot on the lower part of Fig. 3 is in hours and minutes. On this time scale, lithium evaporation should have been observed well before any of the thermocouples detected a significant temperature rise.
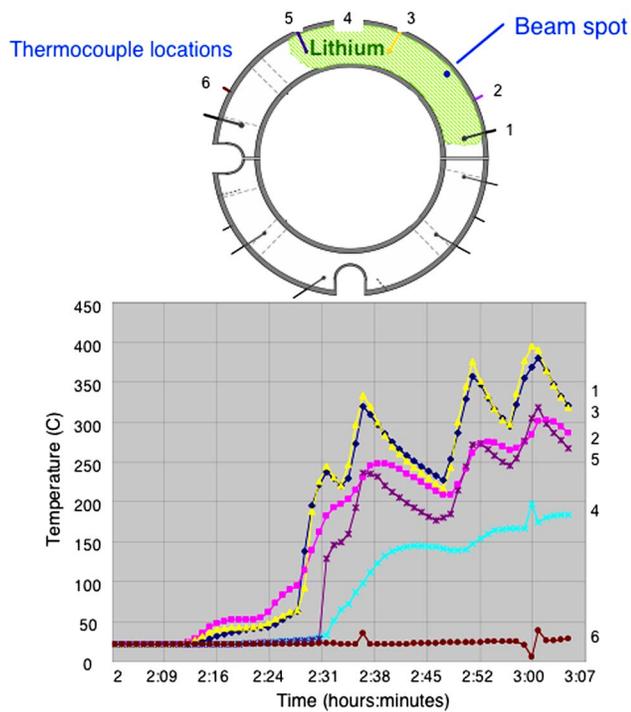
FIG. 3. (Color online) Schematic of CDX-U limiter tray with thermocouple locations (above) and plot of tray temperatures as a function of time during e-beam lithium evaporation (below). The curves on the graph are labeled by the corresponding thermocouple numbers.

Instead, the temperatures measured by thermocouples 1 and 3 were well above 300 °C before significant lithium evaporation was observed with the QDM. The three large peaks in Fig. 3 reflect the times the e-beam was turned off after sufficient lithium evaporation to take a plasma shot. The two uppermost curves represent the signals from these thermocouples, and the lithium becomes molten at their locations at the same time. The way they respond to the e-beam heating cycles suggests that conduction alone is not transporting heat from the point of impact to the sensor location. A similar temporal response is observed with the centrally located thermocouple farthest from the e-beam spot (5), although with a time delay. The two edge thermocouples (2 and 4), however, have a different time behavior that is more indicative of the stainless steel tray material than the liquid lithium.

Measurements with visible and infrared cameras (Fig. 1) provided evidence for the major role convection played in dissipating the e-beam power. Lithium motion was clearly visible at slow standard video (tens of hertz) framing rates, and the infrared images showed that the large temperature gradients expected from conductive heat transport alone were not present.[6]

The mechanism that is driving the convection is believed to be a combination of the $j \times B$ force, arising from the current due to the e-beam and the imposed vertical field, and the Marangoni effect.[9] The latter is related to the dependence of the surface tension on the temperature. This imposes the following boundary condition:
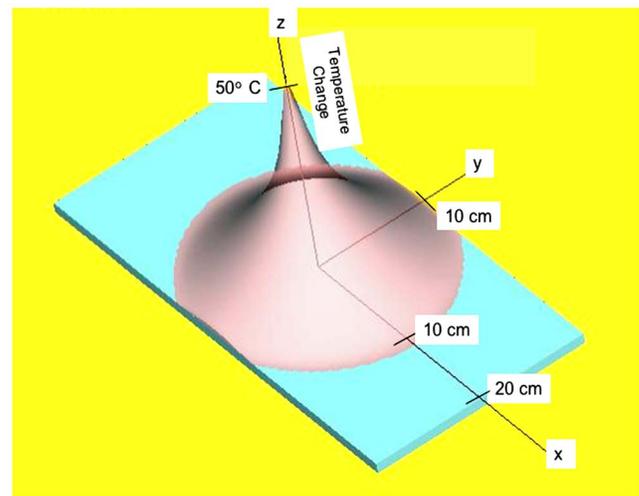

FIG. 4. (Color online) Temperature distribution in liquid lithium resulting from Marangoni effect during e-beam heating. Convection keeps the peak at only 50 °C above its initial value.

$$\nu \mathbf{V}'_n|_{\text{surface}} = \frac{d\sigma(T)}{dT} \nabla_s T. \tag{1}$$

In Eq. (1), $\mathbf{V}'_n$ is the derivative of the fluid velocity normal to the surface, and σ is the surface tension. The viscosity ν for liquid lithium at 300 °C is about 5.6×10^{-4} Pa s, and the following is the associated temperature derivative of the surface tension:

$$\frac{d\sigma(T)}{dT} \approx -1.6 \times 10^{-4} \left[\frac{\text{N}}{\text{m °K}} \right] \tag{2}$$

The importance of the Marangoni effect then becomes evident. The velocity of the liquid lithium surface in the presence of temperature gradients can be estimated as follows:

$$\mathbf{V} = \frac{1}{\nu} \frac{d\sigma(T)}{dT} \nabla_s T d, \tag{3}$$

$$\mathbf{V} = 0.12 \nabla_s T d. \tag{4}$$

The thickness of the viscous boundary layer d is approximately $1.8 \times 10^{-3} \sqrt{t}$, where t is the time in seconds. Without Marangoni convection, the temperature in the e-beam spot exceeds 1000 °C in a fraction of a second, creating a temperature gradient of 10^5 °K/m . Because of the Marangoni effect, however, this condition results in a fluid velocity of 10 m/s, which can efficiently transfer heat out of the region.

Figure 4 is a temperature contour plot from a calculation for an e-beam spot on a 20 cm long section of the 10 cm wide CDX-U liquid lithium limiter tray. Its actual curvature was not simulated for simplicity, but the basic features of the Marangoni effect are clear. The plot represents a time that is long compared to the subsecond interval over which rapid heating is expected without convection. In that case, the temperature distribution would be a sharp and rapidly growing spike. Instead, a modest peak occurs that is only 50 °C above the starting temperature of the liquid lithium. It is kept from exceeding this value by the Marangoni convection, which
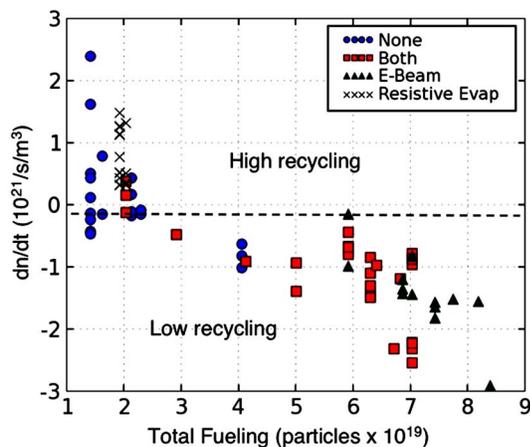
FIG. 5. (Color online) Time derivative of plasma density (dn/dt) as a function of plasma fueling for high and low recycling conditions.

distributes the heat over a lithium volume that increases with time. The temperature distribution is thus a cone with a base that broadens as the heating continues.

High local temperatures are thus not sustained, as a balance between the fluid velocity driven by the surface tension and the temperature gradient is established. This was observed in CDX-U, where the local temperature of the e-beam spot was limited, and the heat was readily distributed to the bulk of the lithium. Furthermore, a velocity of 10 m/s is typical for liquid first wall reactor concepts.[1] Since this is comparable to the fluid flows driven by the Marangoni effect, it might contribute to the handling of high power densities in future fusion devices.

IV. PLASMA PERFORMANCE WITH LITHIUM PFCs

Among the key indicators of changes in recycling is the behavior of plasmas to fueling. There were two external sources of plasma fueling, as indicated in Fig. 1. One is a standard gas injector. This is a commercial Veeco PV-10 piezoelectric valve, connected to a tube that enters the top of the vacuum vessel. The other external fueling source is a supersonic gas injector (SGI).[10] This consists of a graphite Laval nozzle attached directly to a Veeco PV10 valve, so fueling experiments can be performed with a time response on the order of 1 ms. Furthermore, the advantage of the SGI is that unlike the standard gas injector, the nozzle can be moved close to the plasma. To fuel CDX-U discharges, the nozzle tip was located within 1 cm of the last closed flux surface. The fueling was quantified from the duration of the valve opening and the measured throughput of the SGI.[10]

A microwave interferometer was used to measure the time evolution of the line-averaged density (dn/dt) after the termination of SGI fueling.[11] A positive dn/dt indicates that the plasma is still being fueled, whereas a negative dn/dt means that the density is being pumped out. In the present paper, we report this quantity as a function of the plasma fueling. Figure 5 shows the relationship between dn/dt and discharge fueling for four cases. They are plasmas without lithium-coated PFCs, PFCs with lithium coatings from elec-

tron beam (e-beam) and resistive oven evaporation individually, and PFCs coated with lithium from both techniques applied simultaneously.

For plasmas without lithium PFCs, dn/dt increases or remains unchanged after SGI fueling is terminated. This is consistent with continued fueling from high recycling PFCs. Coating the PFC's with resistive oven evaporation alone also resulted in either a flat or rising dn/dt after the end of SGI fueling. This is attributed to the relatively modest rate of lithium deposition (10 nm/min), which was inadequate for maintaining an active lithium surface in the presence of a partial pressure of water in the mid-10^{-8} Torr range.

With PFC coatings from the e-beam alone, or when combined with resistive oven evaporation, dn/dt consistently decreases after SGI fueling terminates. This is attributed to the low recycling lithium PFC conditions achieved with e-beam evaporation. Unlike resistive oven evaporation, 100 nm of lithium can be deposited with the e-beam in less than a minute prior to the discharge. Furthermore, the e-beam liquefied the lithium in the limiter tray for the reasons discussed in Sec. III. This provided an additional 600 cm^2 of a liquid lithium PFC that did not exist with the resistive oven evaporator.

Further evidence of particle pumping with low recycling lithium PFCs is provided when the fueling is increased. The duration of the SGI pulse was extended significantly, as shown in Fig. 5. However, dn/dt remained negative after the termination of SGI fueling, which is indicative of the high particle pumping capability of lithium PFCs. From the dn/dt measurements, a particle pumping rate on the order of 10^{21} particles/s can be deduced. This is comparable to the values achieved in TFTR supershots with lithium-coated PFCs,[12] but with an active lithium surface area that was two orders of magnitude smaller in CDX-U.

Spectroscopic measurements of deuterium and light impurities also provided information on the effects of liquid lithium PFCs on CDX-U plasmas. The primary instruments for these observations were filterscopes,[13] which were detectors equipped with interference filters for a variety of visible lines. The main impurities in CDX-U discharges were oxygen and carbon, and their emission levels were reduced by an order of magnitude in liquid lithium limiter plasmas. This dramatic reduction in impurities provided some of the earliest and most conspicuous evidence that lithium PFCs had a significant effect on CDX-U discharges, and it has been described in detail elsewhere.[8,14,15]

The change in the deuterium-alpha (D_α) emission was used to obtain an estimate of the reduction in recycling with lithium PFCs. Measurements were made with a filterscope viewing the CDX-U center stack through a D_α filter. For plasmas without liquid lithium in the limiter tray, the level of this emission was about a factor of 3 higher than for discharges with liquid lithium limiter.[8,14,15] The recycling coefficient (R) for a plasma limited on a tray without lithium is assumed to be unity. The ratio of the filterscope signals for this discharge and another limited with liquid lithium then means that R is about 0.33 in the latter case.

The deuterium-alpha emission data, however, have to be corrected for differences in the edge parameters. These were

measured with a triple Langmuir probe, and regardless of whether or not there was a liquid lithium limiter, the edge plasma density was about 1×10^{12} cm^{-3}. The edge electron temperatures were different, however. In the absence of a liquid lithium limiter, the edge temperature was about 20 eV. With a liquid lithium limiter, on the other hand, the edge temperature was about ten eV higher at the last closed flux surface. The rise in electron temperature was used in the modeling that compensated for the associated increase in deuterium-alpha emission.[16–18] This introduces about a ten percent correction, so R is closer to 0.3 for liquid lithium limiter plasmas.

Measurements on the PISCES-B linear-edge-plasma simulator have shown that all of the incident deuterium ions can be taken up by liquid lithium, until it is volumetrically converted entirely to lithium deuteride.[3] A recycling coefficient of 0.3 is thus possible in the presence of the liquid lithium in CDX-U. This is the lowest value of R observed to date in a magnetically confined plasma, and it corresponds to discharges that are, for the first time, not dominated by wall fueling.[11] This condition was associated with a dramatic improvement in energy confinement time, or τ_E.[7] This parameter can be defined as follows:

$$\tau_E = \frac{W_{\text{kinetic}}}{\left(- \dfrac{d\psi_{\text{edge}}}{dt} I_p - P_{\text{mag}} - P_{\text{kinetic}} \right)}. \quad (5)$$

Here, W_{kinetic} is the kinetic energy stored in the plasma, and V_{edge} is the surface voltage:

$$V_{\text{edge}} = \frac{d\psi_{\text{edge}}}{dt}. \quad (6)$$

The time derivatives of both the magnetic stored energy (P_{mag}) and the stored kinetic energy (P_{kin}) must be evaluated in the τ_E calculation, since capacitor banks are discharged to provide the Ohmic heating power on CDX-U.

The determination of τ_E depended on equilibria reconstructed with the Equilibrium and Stability Code (ESC).[19] The reconstructions were constrained by measurements from magnetic probes, calibrated using a new response function technique to deal with the nonaxisymmetric eddy currents that are a particular concern for the short CDX-U discharges.[20] A compensated diamagnetic loop (Fig. 1) was used together with the magnetic reconstruction of the plasma boundary to obtain the stored plasma kinetic energy. The point when the time derivative of the magnetic stored energy was zero was determined using ESC. This was close to the peak of the plasma current, and by calculating the poloidal flux at this time with ESC, the surface voltage was obtained.

The τ_E values deduced from the diagnostic measurements and the quantities derived with ESC were in the range of 5 to 6 ms for plasmas with active lithium PFCs. These are discharges with a liquid lithium tray limiter and/or lithium deposited on PFCs immediately preceding the shot. In plasmas prior to the use of lithium PFCs, confinement times were typically about 1 ms, or a factor of 6 lower.[21] It is informative to compare the lithium PFC results on CDX-U with the predictions from ITER98P(y,1) scaling.[22] This is because it
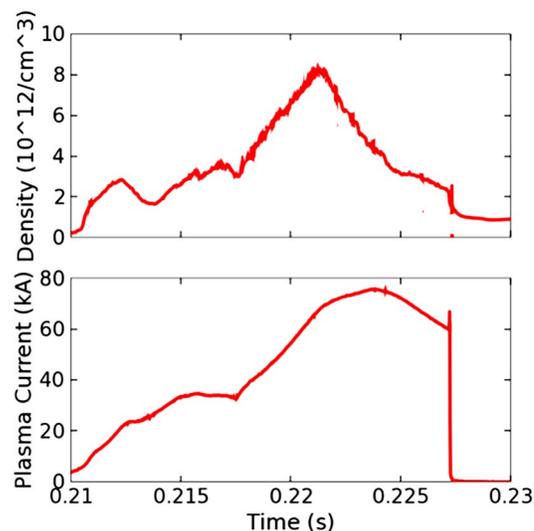

FIG. 6. (Color online) Time dependence of plasma density (upper trace) and current (lower trace) for a low recycling plasma. The density starts decreasing at the end of the SGI pulse, but the current continues to rise.

includes results from the Small Tight Aspect Ratio Tokamak (START),[23] which was also a spherical tokamak and comparable in size to CDX-U. The τ_E values achieved with lithium PFCs exceed ITER98P(y,1) ELMy H-mode scaling by nearly threefold, and represent the largest enhancement in energy confinement time ever observed in an Ohmically heated tokamak.

Achievement of high confinement is consistent with the plasma fueling results. The energy confinement times were determined when the plasma current was at a maximum. In the lithium PFC plasmas with low recycling, this occurred 1 to 2 ms after the termination of the SGI pulse (Fig. 6). This meant that the discharge was sustained only by the particles already in the plasma, and not from any external fueling.

The conditions for high confinement predicted for the low recycling regime are thus potentially satisfied.[24] The absence of an external particle source eliminates the edge mixing that occurs with high recycling, and creates a new region with potentially improved confinement. In this so-called D-region, ambipolarity dictates that the best confined plasma component determine the energy losses, and they are not as dependent on thermal conduction as in the core region.

There is already experimental evidence for improved edge conditions in CDX-U. In addition to higher edge electron temperatures, Langmuir probe measurements for low recycling plasmas also indicated that the temperature gradients became steeper, indicating less collisionality in the scrape-off region. While core fueling with either pellet or neutral beam injection could not be explored in CDX-U, it may be that low recycling alone provided enough particle control to establish high confinement plasmas.

V. EFFECT OF LIQUID LITHIUM ON MHD INSTABILITIES

Among the more conspicuous features of CDX-U liquid lithium limiter discharges was their stability against MHD
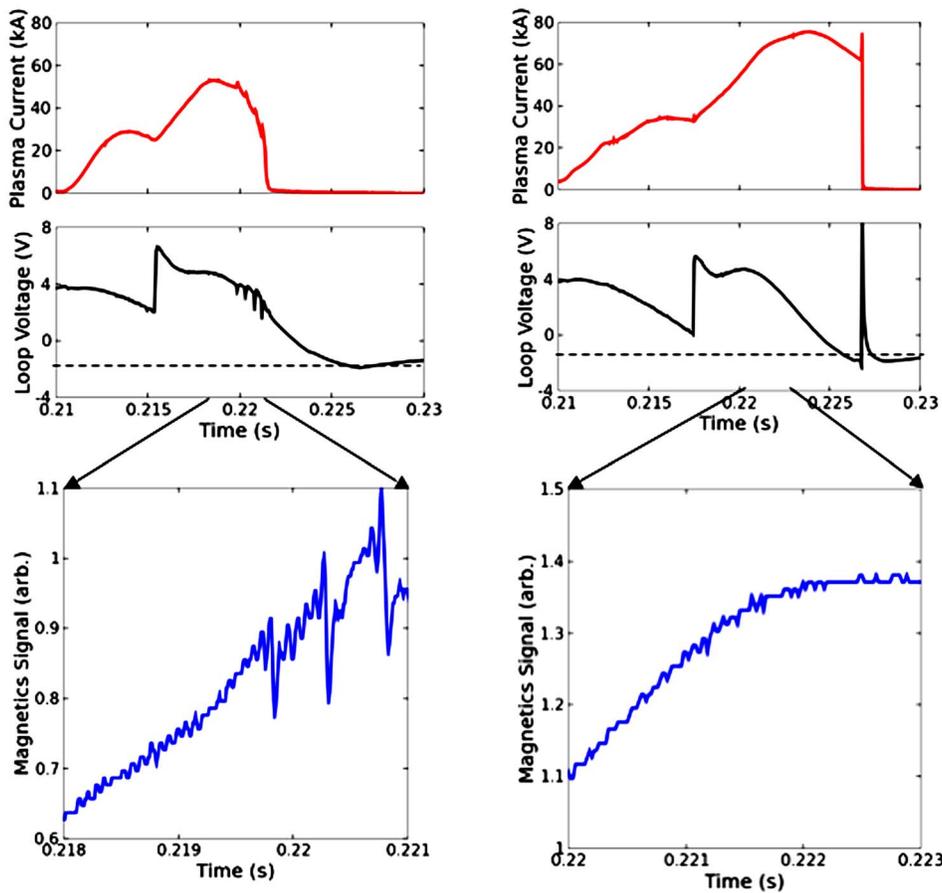
FIG. 7. (Color online) Comparison of plasma current, loop voltage, and magnetic sensor (Mirnov coil) signal for plasma without (left) and with (right) lithium PFC.

modes. Prior to operation with liquid lithium limiters, plasmas often exhibited what were surmised to be resistive MHD modes. Measurements with a soft x-ray detector array and external magnetic pickup coils showed modes with toroidal mode number $n=1$ and poloidal mode number $m=1$, 2, or 3 that grew in amplitude until an internal reconnection event (IRE) occurred.[25] In plasmas with liquid lithium limiters, however, there was no evidence of MHD activity.

Two discharges from the last period of CDX-U operations are compared in Figure 7. The left-hand panels show the plasma current, loop voltage, and signal from one of the external magnetic sensors for a discharge prior to the introduction of lithium into the limiter tray, and the right-hand panels depict the same parameters for a plasma limited with liquid lithium. In each case, the plasma current trace reflects the two phases of CDX-U discharges. Capacitor banks supply the Ohmic heating solenoid for driving the plasma current, and they are fired twice during each CDX-U shot. The second discharge of the capacitors is timed to occur after the plasma current reaches its first peak, and this happens later in the shot with the liquid lithium limiter.

Without the liquid lithium limiter, the plasma current reaches its maximum at about 55 kA. Spikes then appear, correlated with clear drops in the loop voltage signal. The magnetic sensor signal has the characteristic signatures of growing MHD modes that terminate with IREs, and they coincide with the discontinuities in the other traces. The discharge ends after about 11 ms, while the loop voltage is still approximately 2 V.

The liquid lithium limiter discharge is quite different. The maximum plasma current is over 40% higher, or nearly 80 kA. This occurred when the loop voltage was only 0.5 V, or about a factor of 10 lower than the value at the peak plasma current for the discharge without the liquid lithium limiter. The liquid lithium limiter plasma also lasted for 17 ms, which is over 50% longer, and no evidence for MHD activity was present in any of the signals.

The absence of MHD instabilities is consistent with ESC equilibrium reconstructions for the liquid lithium limiter discharge, as the safety factor q was everywhere above 1. A direct measurement of the plasma current profile was not available, and a parabolic shape for it was assumed. To check its validity, the following test was conducted.[26] In the final CDX-U experiments, the center stack was also coated with lithium by evaporation to provide an additional low recycling plasma-facing surface. When the plasma is in contact with the center stack, there is significant lithium line emission, and this was monitored with a filterscope equipped with a Li I interference filter. If this emission drops while the plasma current is still increasing, it means that the plasma has detached from the center stack. This is illustrated in Fig. 8. The equilibria reconstructed with ESC also show detachment from the center stack at a specific time. The shape of the plasma current profile was adjusted until the calculated
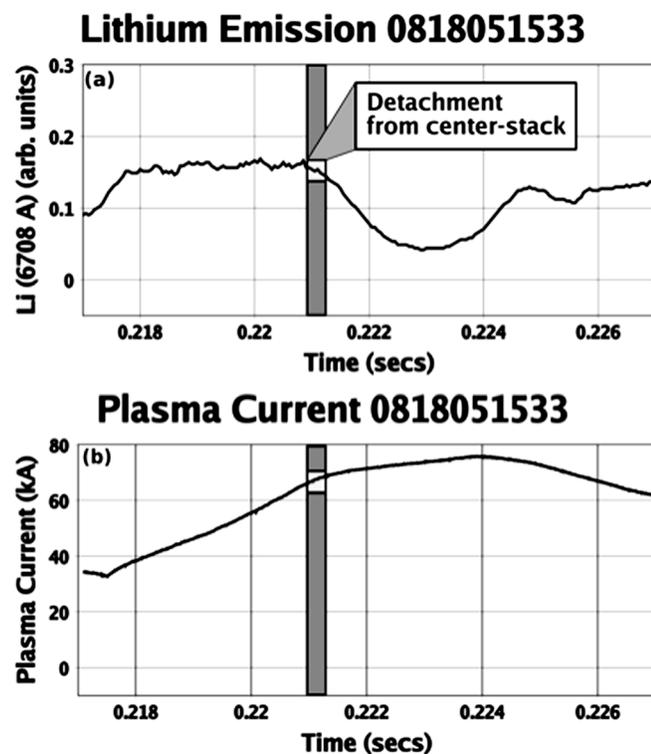
FIG. 8. Time evolution of visible lithium emission from CDX-U center stack (upper plot) and plasma current (lower plot) showing point of plasma "detachment" from center stack.

FIG. 9. (Color online) Computer rendering (left) and photograph of actual components (right) showing conducting shell inside LTX vacuum vessel.

detachment time coincides with the experimental value, and the best fit was for a parabola with a minimum value of q greater than 1.

Because of the short duration of CDX-U plasmas, we are unable to give a definitive reason why central q remains above 1. One reason could be that the evolution of q was slower, and q did not fall below 1 because of the higher temperature in low recycling CDX-U plasmas. Doppler broadening measurements of the carbon impurity line emission suggested that the ion temperature did increase in low recycling plasmas. The lowered resistivity associated with these hotter plasmas means that the current penetration time is longer, so the central q remains above 1 throughout the discharge.

Another reason could be a more flat temperature profile, associated with the lowered recycling and the hotter edge mentioned earlier. In that case, the tendency toward current peaking would be reduced. The Lithium Tokamak Experiment (LTX), described in the next section, will resolve this uncertainty. This successor to CDX-U will have plasmas with longer flattops, and a Thomson scattering diagnostic for electron temperature profile measurements. With the efficient core fueling capability (e.g., neutral beam injection) planned for LTX, the flat temperature profiles predicted for the lithium wall regime are expected to be achieved.

VI. SUMMARY AND FUTURE PLANS

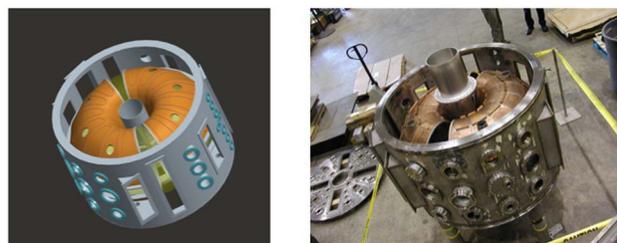The final phase of CDX-U experimental research revealed several significant features of liquid lithium as a plasma-facing component. The highest enhancement in energy confinement time ever observed over scaling predictions for Ohmic plasmas was achieved. A substantial reduction in impurities was also measured, and the absence of resistive MHD instabilities could be attributable to the associated suppression of impurity influx. In addition, the testing of lithium evaporation with an electron beam showed that convective flows efficiently dissipate heat in liquid lithium. This property of lithium suggests its potential for applications in which high power handling is required.

It should also be noted that the CDX-U experiments demonstrated that extensive handling of liquid lithium could be performed practically and safely. Several liters of molten lithium were injected into the CDX-U vacuum vessel over the course of four limiter tray loadings, and this was done without incident. After each run, the lithium in the limiter tray was first passivated with ambient air flowing through the vacuum vessel, and this was shown to be sufficient for the safe removal of each tray section for cleaning and refurbishing.

While the CDX-U experiments were promising, they had several limitations. First, while a substantial fraction of the plasma facing components was covered with lithium, only that in the limiter tray was liquefied. Discharges were limited by the center stack and the bottom tray. There was a solid lithium coating on the center stack during the last CDX-U run, but only the tray provided a true liquid lithium limiter surface. Furthermore, equilibrium reconstructions constrained by magnetic diagnostics were reasonably robust, but they were limited by the lack of direct plasma profile measurements.

These issues will be addressed in LTX, which is under construction at the Princeton Plasma Physics Laboratory (Fig. 9). The LTX reuses the CDX-U vacuum vessel, but has a conformal, conducting shell inside it that almost completely encircles the plasma. The shell is made of copper approximately 1 cm thick, and it has an explosively bonded stainless steel liner on its plasma-facing surface. Lithium will be evaporated onto the stainless steel, which does not react with it, and the copper permits uniform heating to a temperature where the lithium can be kept molten. A key diagnostic for LTX that was unavailable on CDX-U will be a multipoint Thomson scattering system for electron density and temperature profiles. These features will permit LTX to investigate the stable, flat electron temperature profile regime theoretically predicted for lithium wall tokamaks, and first plasma is planned for mid-2007.

[1] M. A. Abdou, A. Ying, N. Morley *et al.*, Fusion Eng. Des. **54**, 181 (2001).

[2] G. Vendryes, Ann. Rev. Energy **9**, 263 (1984).

[3] M. J. Baldwin, R. P. Doerner, S. C. Luckhardt, and R. W. Conn, Nucl. Fusion **42**, 1318 (2002).

[4] D. K. Mansfield, D. W. Johnson, B. Grek *et al.*, Nucl. Fusion **41**, 1823 (2001).

[5] S. I. Krasheninnikov, L. E. Zakharov, and G. E. Pereverzev, Phys. Plasmas **10**, 1678 (2003).

[6] R. Kaita, R. Majeski, R. Doerner, T. Gray, H. Kugel, T. Lynch, R. Maingi, D. Mansfield, V. Soukhanovskii, J. Spaleta, J. Timberlake, and L. Zakharov, "Extremely low recycling and high power density handling in CDX-U lithium experiments," J. Nucl. Mater. (in press).

[7] R. Majeski, R. Doerner, T. Gray, R. Kaita, R. Maingi, D. Mansfield, J. Spaleta, V. Soukhanovskii, J. Timberlake, and L. Zakharov, Phys. Rev. Lett. **97**, 075002 (2006).

[8] R. Majeski, R. Kaita, M. Boaz *et al.*, Fusion Eng. Des. **72**, 121 (2004).

[9] C. E. Brennan, *Fundamentals of Multiphase Flow* (Cambridge University Press, New York, 2005), p. 66ff.

[10] V. Soukhanovskii, H. W. Kugel, R. Kaita, R. Majeski, and A. L. Roquemore, Rev. Sci. Instrum. **75**, 4320 (2004).

[11] T. Gray, R. Kaita, R. Majeski, J. Spaleta, and J. Timberlake, Rev. Sci. Instrum. **77**, 10E901 (2006).

[12] R. Budny, D. Coster, D. Stotler, M. G. Bell, A. C. Jones, and D. K. Owens, J. Nucl. Mater. **196–198**, 462 (1992).

[13] R. J. Colchin, D. L. Hillis, R. Maingi, C. C. Klepper, and N. H. Brooks, Rev. Sci. Instrum. **74**, 2068 (2003).

[14] R. Kaita, R. Majeski, M. Boaz *et al.*, J. Nucl. Mater. **337–339**, 872 (2005).

[15] R. Majeski, T. Gray, D. Hoffman *et al.*, Nucl. Fusion **45**, 519 (2005).

[16] L. C. Johnson and E. Hinnov, J. Quant. Spectrosc. Radiat. Transf. **13**, 333 (1973).

[17] R. K. Janev, D. E. Post, W. D. Langer, K. Evans, D. B. Heifetz, and J. C. Weisheit, J. Nucl. Mater. **121**, 10 (1984).

[18] D. P. Stotler, *Proceedings of the 16th International Conference on Fusion Energy, Montreal, 7–11 October 1996* (IAEA, Vienna, 1977), Vol. 2, p. 633.

[19] L. E. Zakharov and A. Pletzer, Phys. Plasmas **6**, 4693 (1999).

[20] J. Spaleta, L. Zakharov, R. Kaita, R. Majeski, and T. Gray, Rev. Sci. Instrum. **77**, 10E305 (2006).

[21] T. Munsat, P. C. Efthimion, B. Jones, R. Kaita, R. Majeski, D. Stutman, and G. Taylor, Phys. Plasmas **9**, 480 (2002).

[22] ITER Physics Basis Editors, Nucl. Fusion **39**, 2137 (1999).

[23] O. J. W. F. Kardaun, *Proceedings of the 18th IAEA Fusion Energy Conference, Sorrento, 2000* (IAEA, Vienna, 2001), CD-ROM file ITERP/04.

[24] L. E. Zakharov, N. N. Gorelenko, R. B. White, S. I. Krasheninnikov, and G. V. Pereversev, Fusion Eng. Des. **72**, 149 (2004).

[25] M. Ono, D. Stutman, Y. S. Hwang *et al.*, *Proceedings of the 16th IAEA Fusion Energy Conference, Montreal, 1996* (IAEA, Vienna, 1997), IAEA-F1-CN-64/C2-2.

[26] J. Spaleta, Ph.D. thesis, Princeton University, 2006.